HHS Public Access

Author manuscript

Biomater Sci. Author manuscript; available in PMC 2020 November 19.

Published in final edited form as:

Biomater Sci. 2019 November 19; 7(12): 5338–5349. doi:10.1039/c9bm00348g.

Engineering Hydrogels with Affinity-Bound Laminin as 3D Neural Stem Cell Culture Systems

Daniela Barros[1,2,3], **Eduardo Conde-Sousa**[1,2], **Andreia M. Gonçalves**[1,2,3,6], **Woojin M. Han**[4,5], **Andrés J. García**[4,5], **Isabel F. Amaral**[1,2,6,*], **Ana P. Pêgo**[1,2,3,6,*]

[1]i3S - Instituto de Investigação e Inovação em Saúde, Universidade do Porto (UPorto), Portugal

[2]INEB - Instituto de Engenharia Biomédica, UPorto, Portugal

[3]ICBAS - Instituto de Ciências Biomédicas Abel Salazar, UPorto, Portugal

[4]Parker H. Petit Institute for Bioengineering and Biosciences, Georgia Institute of Technology, Atlanta, Georgia, USA

[5]George W. Woodruff School of Mechanical Engineering, Georgia Institute of Technology, Atlanta, Georgia, USA

[6]FEUP - Faculdade de Engenharia, UPorto, Portugal.

Abstract

Laminin incorporation into biological or synthetic hydrogels has been explored to recapitulate the dynamic nature and biological complexity of neural stem cell (NSC) niches. However, the strategies currently explored for laminin immobilization within three-dimensional (3D) matrices do not address a critical aspect influencing cell-matrix interactions, which is the control over laminin conformation and orientation upon immobilization. This is a key feature for the preservation of the protein bioactivity. In this work, we explored an affinity-based approach to mediate the site-selective immobilization of laminin into a degradable synthetic hydrogel. Specifically, a four-arm maleimide terminated poly(ethylene glycol) (PEG-4MAL) macromer was functionalized with a mono-PEGylated recombinant human N-terminal agrin (NtA) domain, to promote high affinity binding of laminin. Different NtA concentrations (10, 50 and 100 μM) were used to investigate the impact of NtA density on laminin incorporation, hydrogel biophysical properties, and biological outcome. Laminin was efficiently incorporated for all the conditions tested (laminin incorporation > 95%), and the developed hydrogels revealed mechanical properties (average storage modulus (G') ranging from 187 to 256 Pa) within the values preferred for NSC proliferation and neurite branching and extension. Affinity-bound laminin PEG-4MAL hydrogels better preserve laminin bioactivity, compared to unmodified hydrogels and hydrogels containing physically entrapped laminin, this effect being dependent on NtA concentration. This was evidenced by the 10 μM NtA-functionalized PEG-4MAL gels incorporating laminin that support

*Corresponding authors: **Isabel Freitas Amaral, Ph.D.,** i3S – Instituto de Investigação e Inovação em Saúde, Universidade do Porto, Rua Alfredo Allen, 208, 4200-135 Porto, Portugal, Tel. +351 22 408 800, iamaral@ineb.up.pt, **Ana Paula Pêgo, Ph.D.,** i3S – Instituto de Investigação e Inovação em Saúde, Universidade do Porto, Rua Alfredo Allen, 208, 4200-135 Porto, Portugal, Tel. +351 22 408 800, apego@i3s.up.pt.

Conflicts of Interest

There are no conflicts of interest to declare.

enhanced human NSC proliferation and neurite extension, compared to the latter. Overall, this work highlights the potential of the proposed engineered matrices to be used as defined 3D platforms for the establishment of artificial NSC niches and as extracellular matrix-mimetic microenvironments to support human NSC transplantation.

Keywords

Laminin; Affinity-binding; Hydrogel; Stem cell niche; Neural stem cells

1. Introduction

Neural stem cells (NSC) hold great potential for application in regenerative medicine and tissue engineering, specifically for the treatment of central nervous system (CNS) disorders (*e.g.* traumatic brain and spinal cord injury and neurodegenerative diseases, such as Parkinson's and Alzheimer's disease) [1–3]. NSC reside within a dynamic and complex microenvironment, the NSC niche, where cell-cell interactions and local microenvironmental cues, including those from neighboring cells, humoral factors and extracellular matrix (ECM), regulate stem cell behavior [4–6]. However, the intrinsic regulatory mechanisms allowing NSC to integrate this complex array of signals remain poorly understood, as the traditional culture systems are unable to recapitulate several important features of these microenvironments [7]. Therefore, the development of new platforms providing a better understanding of the role of different niche components on the modulation of NSC fate is highly desirable. This will be highly advantageous to better understand and overcome some of the main drawbacks limiting the efficacy of current stem cell-based therapies. These limitations include low cell survival, lack of control of cell fate, and poor cell engraftment within the host tissue after transplantation [8]. Different three-dimensional (3D) cell culture systems, including spheroids, porous scaffolds and hydrogels [9, 10], have been explored. These platforms replicate some of the physical and chemical elements of the native stem cell niche and provide valuable insights into cell physiology and interactions with the surrounding microenvironment. Among the different platforms explored, hydrogels constitute the most widespread option, as they are well-defined and tunable matrices that share many key physical properties with native ECM [7], including high-water content, and permeability and elasticity resembling those of soft tissue microenvironments [11, 12]. Indeed, different studies already explored both natural and synthetic polymer-based hydrogels mimicking critical aspects of NSC niches [13–16]. However, their use as permissive microenvironments for cell culture and transplantation is still a challenge. One of the main caveats is related with the inability to control cell spatial organization within the developed matrices, as this is highly dependent not only on the dynamic modulation of cell-cell interactions but also cell-matrix interactions [4–7]. In this sense, in the last few years the use of hybrid hydrogels, which combine the bioactivity and the dynamic responsiveness of natural proteins, with the tunable and reproducible structural and mechanical features provided by synthetic polymers, have been the focus of significant research [12].

Laminin has a key role in the modulation of NSC behavior, including cell adhesion and viability [17], and neuronal outgrowth and migration [18–20]. Furthermore, laminin has other paramount roles in CNS homeostasis, such as synapse function and stability [21, 22]. This makes this heterotrimeric glycoprotein highly attractive for the design of NSC niche microenvironments. Indeed, some works already explored laminin immobilization onto different biological and synthetic materials [23]. However, the non-selective nature of the immobilization strategies explored to date (*i.e.* physical entrapment or non-selective covalent immobilization) prevents the control over laminin orientation and conformation upon immobilization. This may compromise the exposure of crucial laminin bioactive epitopes and consequently, limit its ability to modulate cellular behavior, making these matrices ill-suited to get insight for controlled studies of cell-laminin interactions. Therefore, laminin immobilization strategies that assure both conformation and bioactivity are highly desirable. To fulfill these requirements, we previously proposed an affinity-based approach for laminin immobilization [24, 25], which takes advantage of the native high-affinity interaction (dissociation constant (K_D) = 5 nM) between laminin and the human N-terminal agrin (hNtA) domain [26, 27]. The agrin-binding site within laminin is localized in the central region of its coiled-coil domain and maps to a sequence of 20 conserved residues within the γ1 chain [27, 28]. Interestingly, this interaction requires a coiled-coil conformation of the agrin-binding site [28]. Using self-assembled monolayers, we showed that the site-selective immobilization of laminin better preserves its bioactivity, when compared to non-selective covalent immobilization approaches. This immobilization method translated in an enhanced ability of laminin to polymerize and mediate human NSC (hNSC) adhesion and spreading [24]. Consequently, hNtA was herein explored for attaining the site-selective immobilization of laminin within a degradable synthetic hydrogel. A four-arm maleimide terminated poly(ethylene glycol) (PEG-4MAL) macromer was used as the hydrogel base material (Fig. 1), due to excellent cytocompatibility and *in vivo* tolerance [29–31], and well characterized biochemical and biophysical properties [31–33]. PEG-4MAL macromer was functionalized with a thiol-containing mono-PEGylated rhNtA (NtA) domain, for the site-selective immobilization of laminin to the hydrogels (Fig. 1). Laminin-111 (at a concentration of 100 μg/mL) was the isoform selected for the development of PEG-4MAL hydrogels with affinity-bound laminin, since it was already shown to successfully promote NSC neuronal outgrowth and differentiation [34–38]. To allow the hNSC 3D culture that would span the time frame of hNSC proliferation and neuronal differentiation, a mix of protease degradable (cysteine-flanked matrix metalloproteinase 2 (MMP2)-sensitive peptide) [39] and non-degradable (PEG-dithiol) cross-linkers was used to mediate, under physiological conditions, the formation of a degradable hydrogel network (Fig. 1).

The 3D synthetic matrices proposed in this work allow the controlled immobilization of laminin while preserving the exposure of key bioactive domains involved in NSC proliferation and neurite outgrowth, which are promoted in the proposed hydrogels. Ultimately, these results highlight the potential of the engineered hydrogels to be used as artificial niches to support hNSC culture, and hopefully, transplantation.

2. Materials and Methods

2.1. Hydrogel components

A four-arm maleimide terminated poly(ethylene glycol) (PEG-4MAL; 40 kDa, > 95% purity, > 90% substitution, Jenkem USA) was chosen as the hydrogel base material. A macromer solution was prepared in 10 mM 4-(2-hydroxyethyl)piperazine-1-ethanesulfonic acid (HEPES) in phosphate buffered saline (PBS, pH 7.4) at a final polymer concentration of 10.0% (w/v). Mono-PEGylated recombinant human N-terminal agrin (NtA) domain was produced as previously described [24]. Laminin-111 from mouse Engelbreth-Holm-Swarm sarcoma (msLn-111) was obtained from Sigma-Aldrich. A cysteine-flanked matrix metalloproteinase-2 (MMP2)-sensitive peptide (Acetyl (Ac)-GD*C*DD**SGESPAY↓YTA**DD*C*DG-Amide (NH_2); 2.1 kDa, > 85% purity, GenScript) and a PEG-dithiol (3.5 kDa, ≥ 95% purity, Jenkem USA) were used as the degradable and non-degradable cross-linkers, respectively.

2.2. Mono-PEGylated rhNtA tethering efficiency

To determine the tethering efficiency of NtA to PEG-4MAL, free/unreacted thiols in the reaction mixture were quantified using the Measure-iT thiol assay kit (Invitrogen) according to the manufacturer's instructions. Briefly, PEG-4MAL was functionalized with the NtA domain (input NtA concentration: 10, 50 or 100 μM) for 15 min in 10 mM HEPES in PBS (pH 7.4). The samples were then mixed with thiol-quantitation reagent in a black 96-well plate and the fluorescence measured (λ_{ex} = 494 nm; λ_{em} = 517 nm) using a microwell plate reader (BioTek® Synergy™ Mx). A calibration curve of glutathione (0 – 55 μM) was used to calculate the concentration of free thiols.

2.3. Preparation of affinity-bound laminin PEG-4MAL hydrogels

A schematic representation of affinity-bound laminin PEG-4MAL hydrogel preparation is presented in Fig. 1. Briefly, PEG-4MAL was first functionalized with the NtA domain (input NtA concentration in the gel:10, 50, or 100 μM) for 15 min in 10 mM HEPES in PBS (pH 7.4). msLn-111 (input laminin concentration in the gel: 100 μg/mL) was then added to the mixture and allowed to bind to NtA for 30 min. Functionalized PEG-4MAL precursors were then cross-linked into a hydrogel by addition of a mix of a MMP2-sensitive peptide and a PEG-dithiol prepared in 10 mM HEPES in PBS (pH 6.5), at different % molar ratios (100:0; 80:20; 50:50; 20:80; 0:100). The cross-linkers were added at a 1:1 molar ratio of cysteine residues on the cross-linkers to remaining maleimide groups on NtA-functionalized PEG-4MAL. Hydrogels were polymerized at 37 °C, 5% CO_2 for 15 min. Unmodified PEG-4MAL gels and PEG-4MAL gels containing entrapped msLn-111 (100 μg/mL) were also prepared and used as controls.

2.4. Laminin incorporation within PEG-4MAL hydrogels

Laminin incorporation within PEG-4MAL hydrogels was quantified by an enzyme-linked immunosorbent assay (ELISA). The hydrogels were prepared as previously described and incubated at 37 °C in 125 μL of PBS (pH 7.4). At day 1 and 7, the supernatant was collected, stored at −80 °C and then analyzed using a mouse laminin ELISA kit (Abcam, ab119572)

according to the manufacturer's instructions. Absorbance values were measured at 450 nm using a microwell plate reader (BioTek® Synergy™ Mx).

2.5. Rheological properties and mesh size estimation of affinity-bound laminin PEG-4MAL hydrogels

The rheological properties of PEG-4MAL hydrogels were characterized using a strain-controlled Kinexus Pro Rheometer (Malvern Instruments Ltd, Malvern, UK) and an 8 mm diameter parallel-plate geometry. Hydrogels for each condition (⊘ 8 mm) were prepared as previously described, and allowed to hydrate in PBS (pH 7.4) at 37 °C for 24 h. The samples were then tested in a humidified environment at physiological temperature (37 °C) and with application of 30% compression (oscillatory measurement gap). Amplitude strain sweeps (0.1 – 100% at 0.1 Hz) were initially performed for each condition to define the linear viscoelastic region (LVR). Frequency sweeps (0.01 – 10 Hz at 1% strain) were then performed and the storage (G'), loss (G") and complex (G*) modulus, as well as the phase angle (δ, °) were determined within the LVR, by averaging all data points acquired from a 0.01 – 1 Hz interval. The relative mesh size (nm) value was estimated using the following equation [40]:

$$\xi = \left(\frac{G'A}{RT}\right)^{-\frac{1}{3}}$$

where G' = storage modulus in Pa, A = Avogadro's constant ($6.022140857 \times 10^{23}$ mol^{-1}), R = gas constant (8.314 $m^3.Pa.mol^{-1}.K^{-1}$), T = temperature (37 °C = 310.15 K).

2.6. Culture of human neural stem cells

Human neural stem cells (hNSC) derived from the NIH approved H9 (WA09) human embryonic stem cell line were purchased from Life Technologies (N7800–200). Cells were expanded according to the manufacturer's protocol on poly(ornithine)/msLn-111-coated tissue coated polystyrene (TCPS) plates (Corning) in expansion medium - StemPro® NSC serum-free medium (SFM; Life Technologies) supplemented with basic fibroblast growth factor (bFGF, 20 ng/mL; Life Technologies) and epidermal growth factor (EGF, 20 ng/mL; Life Technologies).

2.7. Culture of hNSC within affinity-bound laminin PEG-4MAL hydrogels

hNSC were dissociated into single cells using StemPro accutase cell dissociation reagent (Life Technologies) and further suspended in the solution containing laminin-functionalized PEG-4MAL precursors (4×10^6 viable cells/mL). Cell-laden hydrogels were formed by mixing the PEG-4MAL precursor solution containing cells with the MMP2-sensitive peptide and PEG-dithiol cross-linkers, dissolved in 10 mM HEPES in PBS (pH 6.5), at different molar ratios (%), and subsequently incubating the polymerizing gels at 37 °C, 5% CO_2 for 15 minutes. hNSC were initially cultured in expansion medium and then induced to differentiate along the neuronal lineage by growth factor withdrawal. Briefly, at day 2 of culture, the medium was switched to the StemPro NSC SFM media-Neurobasal/B27 (Life Technologies) (1:1) mix, without growth factors. At day 8, half of the medium was replaced

by the StemPro NSC SFM-Neurobasal/B27 (1:3) mix supplemented with 10 ng/mL of brain-derived neurotrophic factor (BDNF; Peprotech) and 500 μM of N^6, 2'-O-Dibutyryladenosine 3', 5'-cyclic monophosphate sodium salt (dibutyril cAMP; Sigma). Half of the medium was changed every other day, up to 14 days. hNSC cultured within unmodified and PEG-4MAL gels containing entrapped msLn-111 (100 μg/mL) were herein used as controls.

2.8. Cell viability

The distribution of viable and dead cells within PEG-4MAL hydrogels was assessed at day 7 of cell culture using a live/dead assay. Cell-hydrogel matrices were rinsed with warm PBS pH 7.4 and incubated with 4 μM calcein AM (Life Technologies) and 6 μM propidium iodide (PI; Life Technologies) at 37 °C for 30 min, for detection of viable and dead cells, respectively. After incubation, the samples were rinsed twice with PBS pH 7.4, transferred to the culture medium, and immediately observed under confocal laser scanning microscopy (CLSM, Leica TCS SP5). Quantitative analysis of live and dead cells was also conducted using immunocytometry (See Supplementary Materials and Methods).

2.9. DNA quantification

The growth of hNSC cultured within PEG-4MAL hydrogels was estimated from total cell number after 7 days of cell culture, determined using the CyQUANT® cell proliferation assay kit (Life Technologies) according to the manufacturer's instructions. Briefly, cells were retrieved from the hydrogels, through sequential incubation with 1.25 mg/mL of collagenase type II (Gibco; 1 h at 37 °C) and StemPro accutase cell dissociation reagent (Life Technologies; 20 min at 37 °C) under stirring (70 rpm). Cells were mechanically dissociated by pipetting, diluted in Glasgow Minimum Essential Medium (GMEM; Life Technologies) supplemented with 10% (v/v) inactivated fetal bovine serum (FBS), centrifuged and the cell pellet stored at −80 °C. The cell pellet was then thawed at room temperature (RT) and incubated with CyQUANT® GR dye/cell lysis buffer. Fluorescence (λ_{ex} = 480 nm; λ_{em} = 520 nm) was measured, after mixing with CyQUANT GR dye, in a microwell plate reader (BioTek® Synergy™ Mx). The total number of cells for each condition was estimated from a standard curve generated with a known amount of hNSC over a range of 50 to 250,000 cells. Cell samples used to generate the standard curve were measured in triplicate. For each condition, hydrogels without cells, cultured in parallel and processed similarly to those with cells, were used as blanks and their background fluorescence values subtracted.

2.10. hNSC neurite outgrowth and phenotypic analysis

The effect of laminin site-selective immobilization on neurite outgrowth and cell phenotype was assessed after 14 days of culture. Samples were processed as whole-mounts for immunofluorescence staining of Nestin (neural stem/progenitor cells), βIII-tubulin (developing and mature neurons) microtubule-associated protein 2 (MAP2; neuronal dendrites and cell bodies), and Tau (mature neurons, axonal marker), as described in Supplementary Materials and Methods, and z-sections covering a thickness of 200 μm or 80 μm were acquired with the CLSM using an HC Plan APO CS 10× / 0.40 NA or HC Plan APO CS 20× / 0.70 NA objective. Neurite outgrowth was assessed in the projected two-dimensional (2D) images stained for βIII-tubulin/DNA using a developed ImageJ script.

Briefly, nuclei were segmented through an Otsu thresholding method, while neurites were segmented through subtraction of the previously identified nucleus, using a Huang thresholding method. Measurements were obtained for total neurite length (μm) and total number of neurites per image.

2.12. Statistical Analysis

Statistical analysis was performed using GraphPad Prism 6 software (San Diego). Sample distribution was initially tested for normality using the Kolmogorov-Smirnov test. Comparisons between three or more groups were performed with one-way ANOVA analysis, followed by the Bonferroni correction for pairwise comparisons or the Dunnett's two-tailed test for comparisons with control conditions. For all analysis, differences were considered significant at $p < 0.05$.

3. Results and Discussion

3.1. PEG-4MAL hydrogels provide independent control of different biochemical and biophysical properties

A hydrogel platform based on a PEG-4MAL macromer (Fig. 1) was selected as the base material for this work, as we have seen it exhibits excellent *in vitro* and *in vivo* biocompatibility with different cell types, including muscle stem cells [31] and pancreatic islets [29]. Moreover, the modular nature of PEG-4MAL hydrogels allows independent control over different biochemical and biophysical properties such as type and density of cell-adhesive ligands, mechanical and structural properties, and protease-dependent degradation [31–33]. Therefore, the use of these matrices is especially advantageous to assess the effect of a particular biochemical or biophysical cue on the modulation of cell behavior. In addition, the biophysical properties of these hydrogels were extensively characterized in several studies from the Garcia group [31–33]. The described properties allowed us to initially define the molecular weight (40 kDa) and the final polymer density (10% (w/v) of the PEG-4MAL macromer), that would result in hydrogels with mechanical properties within the range of values preferred for NSC proliferation (100 – 1000 Pa) and neurite branching and extension (200 – 400 Pa) [41–46].

3.1.1. Control over affinity-bound laminin PEG-4MAL hydrogel degradability is required for hNSC long-term culture—Hydrogel degradability, a critical factor for matrix remodeling, was shown to be essential for *in vitro* cell survival and proliferation within synthetic niches [16, 31, 33] and, therefore, is a key feature to take into consideration when designing cell instructive microenvironments. In this context, the incorporation of protease-sensitive peptide cross-linkers has been widely explored to better control material degradation [39]. Among the different protease-degradable peptides characterized to date, a fast-degrading sequence shown to be relatively specific for MMP2 [39] was used, as this metalloproteinase is expressed at high levels by NSC [47, 48].

The fast gelation kinetics of the thiol-maleimide reaction (Michael-type addition; Fig. 1) may lead to the formation of heterogeneous hydrogels, which in turn can translate into variable cell biological outcomes [49]. Consequently, to increase the pKa of the thiol group

and thereby reduce the availability of the reactive thiolate [49], the di-thiol-containing MMP2-sensitive cross-linker peptide used in this work, was designed to include negatively charged amino acids flanking the thiol-bearing cysteine residue (D*C*DD). This strategy allowed the thorough mixing of the hydrogel precursor solutions prior to use.

The fast-degrading nature of the selected MMP2 sequence, combined with the high levels of MMP2 production by NSC, led us to hypothesize that fully degradable hydrogels might not be able to support the 3D culture of hNSC, up to 14 days. To test this hypothesis, affinity-bound laminin hydrogels cross-linked by addition of a MMP2-sensitive peptide (degradable) and a PEG-dithiol (non-degradable) at different % molar ratios (100:0; 80:20; 50:50; 20:80; 0:100) were evaluated and the combination allowing the hNSC 3D culture that would span the time frame of hNSC proliferation and neuronal differentiation established. hNSC showed a significantly higher number of viable cells, with cellular extensions at day 14 of cell culture, in gels formulated with a combination of degradable and non-degradable cross-linkers, specifically for the 80% MMP2-sensitive peptide to 20% PEG-dithiol cross-linker molar ratio, when compared to fully degradable hydrogels ($p = 0.018$ *vs.* 100:0 cross-linker molar ratio (%); Fig. S1, in Supplementary Data). As such, all subsequent studies were performed using this degradable and non-degradable cross-linkers molar ratio (%).

3.1.2. Mono-PEGylated rhNtA (NtA) mediates efficient site-selective laminin incorporation—Maleimide groups in PEG-4MAL macromer efficiently react with thiol-containing peptides through Michael-type addition [32]. This enables a fine-tuning over ligand incorporation and cross-linking efficiency, ultimately leading to the formation of structurally defined matrices. To favor the site-selective immobilization of laminin, PEG-4MAL was first reacted with a thiol-containing NtA domain (Fig. 1). This domain was tethered onto the PEG-4MAL macromer with high yields, for all the concentrations tested (10, 50 and 100 μM), evidencing a precise control over NtA density (Fig. 2A). The effect of different NtA concentrations on laminin incorporation within hydrogels was then assessed. Efficient laminin incorporation was observed for all the NtA concentrations tested, as evidenced by ELISA results (incorporation efficiency > 95%, determined after 1 and 7 days of incubation in PBS; Fig. 2B). We hypothesize that the lack of significant differences between laminin entrapped *vs.* immobilized can be explained by limitations on protein diffusion imposed by the reduced hydrogel mesh size (20 – 30 nm), which will hinder the diffusion of laminin due to its high hydrodynamic diameter (≅ 42 nm) [50, 51].

As free thiol groups in laminin could also react with maleimide groups from PEG-4MAL and thus contribute to the laminin immobilization into PEG-4MAL hydrogels, the availability of free/unreacted thiols in laminin stock solution (pH 7.4) was assessed. Free thiols were not detected (< 2.75 μM, the lower detection limit of the assay), indicating that the molar ratio of free thiols in laminin was less than 0.22%, and assuring minimal contribution of laminin free thiol groups to laminin incorporation into PEG-4MAL hydrogel.

3.1.3. Laminin-modified hydrogels present mechanical properties within the values preferred for NSC growth and differentiation—Hydrogel mechanical and structural (equilibrium swelling and mesh size) properties have a key role on the modulation of different cellular functions (*e.g.* survival, proliferation, and differentiation) [31–33], as

well as in the stability of the hydrogel *in vivo* [41–46, 52]. The fine control of these properties is, therefore, crucial to direct neural stem cell fate [41, 44–46].

The effect of the binding ligand (NtA) density and laminin incorporation on hydrogel mechanical properties and structure (mesh size) was assessed through rheological studies. All the prepared hydrogels presented Storage modulus (G') > Loss modulus (G") (Table 1), showing that PEG-4MAL has transitioned from a viscous liquid to a gelled state. Moreover, the hydrogels presented a "solid-like" behavior after 24h at 37 °C, as evidenced by the values of phase angle (δ) below 10° (Table 1), meaning that the viscoelastic properties of the hydrogels were stable for the conditions tested.

The covalent immobilization of increasing concentrations of NtA (from 10 to 100 μM) led to a trend for reduced in the storage modulus (G') (Table 1) and to the formation of a slightly looser polymer network, as evidenced by the tendency for larger mesh size values (Fig. 3B). The tethering of NtA reduces the number of maleimide-terminated PEG chains available for cross-linking, thus reducing the number of cross-linking points. This is in an excellent agreement with the trend for a lower stiffness observed with increasing concentrations of NtA (Fig. 3A). Results presented are consistent with previous studies, exploring PEG-diacrylate hydrogels, in which it was shown that the covalent immobilization of laminin through a PEG chain significantly reduces the hydrogel stiffness, as opposed to the physical entrapment of the protein [37].

3.2. Affinity-bound laminin PEG-4MAL hydrogels support hNSC culture and biological function

The potential of PEG-4MAL hydrogels incorporating affinity-bound laminin to support hNSC biological function, namely viability, proliferation, and outgrowth, was subsequently investigated. Laminin incorporation within PEG-4MAL hydrogels using 10 and 50 μM NtA, favored the formation of stiffer hydrogels (Fig. 3A), able to better support hNSC culture for longer periods (up to 14 days). As result, these hydrogels were used to perform the qualitative and quantitative analysis of cell behavior. PEG-4MAL hydrogels unmodified or containing physically entrapped laminin were also prepared and used as controls.

3.2.1. Laminin-modified hydrogels support hNSC survival and proliferation—

To get insight into the effect of controlled immobilization of laminin on hNSC survival and proliferation, cells were cultured for 7 days within degradable PEG-4MAL hydrogels with either entrapped or immobilized laminin. Confocal microscopy showed the presence of live cells widely distributed throughout all hydrogels, often growing as cellular spheroids (Fig. 4A). The quantitative analysis of live/dead cells, assessed by flow cytometry, showed values of average cell viability greater than 75% for all the conditions tested, evidencing the good cytocompatibility of the proposed matrices (Fig. 4B) [53].

In contrast to the physical entrapment of laminin, site-selective immobilization of laminin using 10 μM and 50 μM NtA supported higher hNSC growth compared to unmodified hydrogels, with significantly higher cell numbers being observed in 10 μM NtA - laminin immobilized hydrogels ($p = 0.0180$) (Fig. 4C). An increase in the cell number of 1.5-, 1.9-, 4.2- and 3.1-fold (*vs.* initial cell density - 4×10^4 cells/hydrogel) was observed for

unmodified, laminin entrapped, 10 μM- and 50 μM NtA - laminin immobilized hydrogels, respectively (Fig. 4C). Since laminin retention in PEG-4MAL hydrogels was similar regardless of being physically entrapped or affinity-bounded (Fig. 2B), these results suggest that the site-selective immobilization of laminin through the use of 10 μM of NtA, better preserved the exposure of laminin domains interacting with cell adhesion receptors, as compared to laminin physically entrapped.

3.2.2. Controlled laminin immobilization promotes neurite outgrowth— Laminin presents several bioactive domains with neurite outgrowth promoting ability, and, as a result, plays a key role in mediating NSC migration, differentiation and neurite extension both *in vitro* and *in vivo* [18, 20]. The effect of laminin site-selective immobilization on hNSC neurite outgrowth was assessed after 14 days of culture under differentiation conditions (Fig. 5). A population of cells expressing the neuronal marker βIII-tubulin, with the evident formation of neuronal processes, was observed within 10 μM NtA affinity-immobilized laminin PEG-4MAL hydrogels (Fig. 5A). Differences between the conditions tested were assessed by image processing and quantitative analysis, using ImageJ/Fiji. Total neurite length (μm) and total number of neurites were quantified (Fig. 5B–D). The controlled immobilization of laminin using 10 μM NtA supported a more pronounced neurite extension, compared with any of the other conditions tested, as evidenced by the higher values of total neurite length ($p = 0.0035$ *vs.* Unm; $p = 0.0152$ *vs.* Entrap; Fig. 5B) and total number of neurites ($p = 0.0007$ *vs.* Unm; $p = 0.0079$ *vs.* Entrap; Fig. 5C). The use of 50 μM NtA, despite leading to similar amounts of laminin incorporation (Fig. 2B), resulted in significantly lower values of total neurite length ($p = 0.0056$; Fig. 5C) and total number of neurites ($p = 0.0073$; Fig. 5D) compared to 10 μM NtA affinity-bound laminin. The reduction in neurite outgrowth (Fig. 5C–D) and the reduction in cell number (Fig.4C) observed for cells cultured within hydrogels with 50 μM NtA - immobilized laminin may be related with the inability of the protein to bind the NtA domain, as result of steric effects. The results obtained contrast to previous studies in which no significant differences on neurite outgrowth were observed when laminin was covalently immobilized using a non-selective approach, *vs.* physically entrapped laminin [37]. This gives a good indication that the strategy proposed in this study, indeed, potentiate laminin bioactivity.

Overall, these results clearly demonstrate that the site-selective immobilization of laminin through the use of 10 μM NtA better preserved protein bioactivity in terms of ability to promote hNSC proliferation and outgrowth, when compared to laminin physically entrapped.

3.2.3. Controlled laminin immobilization supports hNSC stemness and neuronal maturation— A more detailed phenotypic analysis was performed at day 14 of cell culture by immunocytochemistry (Fig. 6). At this time point, $Nestin^+$ cells (Fig. 6A) were observed for all the conditions tested, thus evidencing the potential of the proposed hydrogels to support hNSC stemness over time. This is a key feature when envisaging the use of hydrogels for cell transplantation, as they should provide an adequate microenvironment for the maintenance of a pool of NSC, upon transplantation. The ability of the proposed hydrogels to support hNSC neuronal maturation was further assessed using

markers for mature neurons, more specifically MAP2 and Tau. The qualitative analysis of 2D projected CLSM images revealed the presence of differentiated neurons expressing MAP2 and Tau in all the conditions. Yet, axonal extensions staining positively for Tau were more evident in 10 μM NtA affinity-immobilized laminin PEG-4MAL hydrogels, which suggests that these hydrogels are more permissive to hNSC neuronal maturation when compared to unmodified gels and gels containing physically-entrapped laminin, in line with their higher neurite-promoting ability.

4. Conclusion

The present work demonstrates the potential of a PEG-4MAL hydrogel modified with affinity-bound laminin as a dynamic 3D platform enabling NSC proliferation, neuronal differentiation and neurite extension. The proposed strategy allows the oriented and controlled immobilization of laminin, with preservation of protein bioactivity, thus overcoming some of the main drawbacks associated with the currently available strategies (*i.e.* physically entrapment and non-selective covalent immobilization). Moreover, the immobilization approach used in this work is highly versatile, as result of the ability of NtA to bind with high affinity to different laminin isoforms comprising the γ1 chain, which represents more than 50% of the isoforms identified to date. Therefore, the reported 3D matrices can be used for the site-selective immobilization of different laminin isoforms and used for the study of cell-laminin interactions occurring in different stem cell niches and disease contexts. These hydrogels can be also of interest to provide a controlled niche with instructive cues to improve survival, engraftment and long-term function of transplanted stem cells; for the creation of tissue-engineered constructs; and for the development of cell expansion and biomanufacturing systems.

Supplementary Material

Refer to Web version on PubMed Central for supplementary material.

Acknowledgments

Confocal microscopy was conducted at the Bioimaging i3S Scientific Platform, member of the PPBI (PPBI-POCI-01–0145-FEDER-022122), with the assistance of Maria Lázaro. This work was funded by projects NORTE-01–0145-FEDER-000008 and NORTE-01–0145-FEDER-000012, supported by Norte Portugal Regional Operational Programme (NORTE 2020), under the PORTUGAL 2020 Partnership Agreement, through the European Regional Development Fund (ERDF) and FEDER - Fundo Europeu de Desenvolvimento Regional funds through the COMPETE 2020 - Operacional Programme for Competitiveness and Internationalisation (POCI), Portugal 2020; by Portuguese funds through FCT/MCTES in the framework of the project “Institute for Research and Innovation in Health Sciences” (POCI-01–0145-FEDER-007274), and by Santa Casa da Misericordia de Lisboa through project COMBINE (Prémio Neurociências Melo e Castro 1068–2015).

DB was supported by FCT PhD Programs (PD/BD/105953/2014) and Programa Operacional Potencial Humano (POCH), in the scope of the BiotechHealth Program (Doctoral Program on Cellular and Molecular Biotechnology Applied to Health Sciences), Programa FLAD Healthcare 2020 and the project PARES (Prémio Albino Aroso). Eduardo Conde-Sousa was supported by a post-doctoral grant of the project PPBI-POCI-01–0145-FEDER-022122, in the scope of FCT National Roadmap of Research Infrastructures. AJG acknowledges support from the National Institutes of Health (R01 AR062368).

References

[1]. Pluchino S, Zanotti L, Deleidi M, Martino G, Neural stem cells and their use as therapeutic tool in neurological disorders, Brain Res Brain Res Rev 48(2) (2005) 211–9. [PubMed: 15850660]

[2]. Cossetti C, Alfaro-Cervello C, Donega M, Tyzack G, Pluchino S, New perspectives of tissue remodelling with neural stem and progenitor cell-based therapies, Cell Tissue Res 349(1) (2012) 321–9. [PubMed: 22322425]

[3]. Gage FH, Temple S, Neural stem cells: generating and regenerating the brain, Neuron 80(3) (2013) 588–601. [PubMed: 24183012]

[4]. Gattazzo F, Urciuolo A, Bonaldo P, Extracellular matrix: a dynamic microenvironment for stem cell niche, Biochim Biophys Acta 1840(8) (2014) 2506–19. [PubMed: 24418517]

[5]. Lane SW, Williams DA, Watt FM, Modulating the stem cell niche for tissue regeneration, Nat Biotechnol 32(8) (2014) 795–803. [PubMed: 25093887]

[6]. Vishwakarma A, Rouwkema J, Jones PA, Karp JM, The Need to Study, Mimic and Target Stem Cell Niches, in: Vishwakarma A, Karp JM (Eds.), Biology and Engineering of Stem Cell Niches, Elsevier2017.

[7]. Wilson JL, McDevitt TC, Biofunctional Hydrogels for Three-Dimensional Stem Cell Culture, in: Vishwakarma A, Karp JM (Eds.), Biology and Engineering of Stem Cell Niches, Elsevier2017.

[8]. Amer MH, Rose F, Shakesheff KM, Modo M, White LJ, Translational considerations in injectable cell-based therapeutics for neurological applications: concepts, progress and challenges, NPJ Regen Med 2 (2017) 23. [PubMed: 29302358]

[9]. Ruedinger F, Lavrentieva A, Blume C, Pepelanova I, Scheper T, Hydrogels for 3D mammalian cell culture: a starting guide for laboratory practice, Appl Microbiol Biotechnol 99(2) (2015) 623–36. [PubMed: 25432676]

[10]. Technology Platforms for 3D Cell Culture: A User's Guide, John Wiley & Sons Ltd2017.

[11]. Tibbitt MW, Anseth KS, Hydrogels as Extracellular Matrix Mimics for 3D Cell Culture, Biotechnol. Bioeng 103(4) (2009) 655–663. [PubMed: 19472329]

[12]. Barros D, Amaral IF, Pego AP, Biomimetic synthetic self-assembled hydrogels for cell transplantation, Curr Top Med Chem 15(13) (2015) 1209–26. [PubMed: 25858129]

[13]. Lampe KJ, Heilshorn SC, Building stem cell niches from the molecule up through engineered peptide materials, Neurosci Lett 519(2) (2012) 138–46. [PubMed: 22322073]

[14]. Lam J, Carmichael ST, Lowry WE, Segura T, Hydrogel design of experiments methodology to optimize hydrogel for iPSC-NPC culture, Adv Healthc Mater 4(4) (2015) 534–9. [PubMed: 25378176]

[15]. Regalado-Santiago C, Juarez-Aguilar E, Olivares-Hernandez JD, Tamariz E, Mimicking Neural Stem Cell Niche by Biocompatible Substrates, Stem Cells Int 2016 (2016) 1513285. [PubMed: 26880934]

[16]. Madl CM, LeSavage BL, Dewi RE, Dinh CB, Stowers RS, Khariton M, Lampe KJ, Nguyen D, Chaudhuri O, Enejder A, Heilshorn SC, Maintenance of neural progenitor cell stemness in 3D hydrogels requires matrix remodelling, Nat Mater 16(12) (2017) 1233–1242. [PubMed: 29115291]

[17]. Hyysalo A, Ristola M, Makinen ME, Hayrynen S, Nykter M, Narkilahti S, Laminin alpha5 substrates promote survival, network formation and functional development of human pluripotent stem cell-derived neurons in vitro, Stem Cell Res 24 (2017) 118–127. [PubMed: 28926760]

[18]. Luckenbill-Edds L, Laminin and the mechanism of neuronal outgrowth, Brain Res Brain Res Rev 23(1–2) (1997) 1–27. [PubMed: 9063584]

[19]. Powell SK, Kleinman HK, Neuronal laminins and their cellular receptors, Int J Biochem Cell Biol 29(3) (1997) 401–14. [PubMed: 9202420]

[20]. Plantman S, Patarroyo M, Fried K, Domogatskaya A, Tryggvason K, Hammarberg H, Cullheim S, Integrin-laminin interactions controlling neurite outgrowth from adult DRG neurons in vitro, Mol Cell Neurosci 39(1) (2008) 50–62. [PubMed: 18590826]

[21]. Rogers RS, Nishimune H, The role of laminins in the organization and function of neuromuscular junctions, Matrix Biol 57-58 (2017) 86–105.

[22]. Nishimune H, Valdez G, Jarad G, Moulson CL, Muller U, Miner JH, Sanes JR, Laminins promote postsynaptic maturation by an autocrine mechanism at the neuromuscular junction, J Cell Biol 182(6) (2008) 1201–15. [PubMed: 18794334]

[23]. Talovic M, Marcinczyk M, Ziemkiewicz N, Garg K, Laminin Enriched Scaffolds for Tissue Engineering Applications, Advances in Tissue Engineering and Regenerative Medicine 2(3) (2017).

[24]. Barros D, Parreira P, Furtado J, Ferreira-da-Silva F, Conde-Sousa E, Garcia AJ, Martins MCL, Amaral IF, Pego AP, An affinity-based approach to engineer laminin-presenting cell instructive microenvironments, Biomaterials 192 (2019) 601–611. [PubMed: 30509501]

[25]. Barros D, Amaral IF, Pêgo AP, Laminin immobilization, methods and uses thereof, Provisional Patent Application, 2018.

[26]. Mascarenhas JB, Ruegg MA, Winzen U, Halfter W, Engel J, Stetefeld J, Mapping of the laminin-binding site of the N-terminal agrin domain (NtA), EMBO J 22(3) (2003) 529–36. [PubMed: 12554653]

[27]. Denzer AJ, Schulthess T, Fauser C, Schumacher B, Kammerer RA, Engel J, Ruegg MA, Electron microscopic structure of agrin and mapping of its binding site in laminin-1, EMBO J 17(2) (1998) 335–43. [PubMed: 9430625]

[28]. Kammerer RA, Schulthess T, Landwehr R, Schumacher B, Lustig A, Yurchenco PD, Ruegg MA, Engel J, Denzer AJ, Interaction of agrin with laminin requires a coiled-coil conformation of the agrin-binding site within the laminin gamma1 chain, EMBO J 18(23) (1999) 6762–70. [PubMed: 10581249]

[29]. Weaver JD, Headen DM, Aquart J, Johnson CT, Shea LD, Shirwan H, Garcia AJ, Vasculogenic hydrogel enhances islet survival, engraftment, and function in leading extrahepatic sites, Sci Adv 3(6) (2017) e1700184. [PubMed: 28630926]

[30]. Cruz-Acuna R, Quiros M, Farkas AE, Dedhia PH, Huang S, Siuda D, Garcia-Hernandez V, Miller AJ, Spence JR, Nusrat A, Garcia AJ, Synthetic hydrogels for human intestinal organoid generation and colonic wound repair, Nat Cell Biol 19(11) (2017) 1326–1335. [PubMed: 29058719]

[31]. Han WM, Anderson SE, Mohiuddin M, Barros D, Nakhai SA, Shin E, Amaral IF, Pego AP, Garcia AJ, Jang YC, Synthetic matrix enhances transplanted satellite cell engraftment in dystrophic and aged skeletal muscle with comorbid trauma, Sci Adv 4(8) (2018) eaar4008. [PubMed: 30116776]

[32]. Phelps EA, Enemchukwu NO, Fiore VF, Sy JC, Murthy N, Sulchek TA, Barker TH, Garcia AJ, Maleimide cross-linked bioactive PEG hydrogel exhibits improved reaction kinetics and cross-linking for cell encapsulation and in situ delivery, Adv Mater 24(1) (2012) 64-70, 2.

[33]. Enemchukwu NO, Cruz-Acuna R, Bongiorno T, Johnson CT, Garcia JR, Sulchek T, Garcia AJ, Synthetic matrices reveal contributions of ECM biophysical and biochemical properties to epithelial morphogenesis, J Cell Biol 212(1) (2016) 113–24. [PubMed: 26711502]

[34]. Addington CP, Heffernan JM, Millar-Haskell CS, Tucker EW, Sirianni RW, Stabenfeldt SE, Enhancing neural stem cell response to SDF-1alpha gradients through hyaluronic acid-laminin hydrogels, Biomaterials 72 (2015) 11–9. [PubMed: 26340314]

[35]. Addington CP, Dharmawaj S, Heffernan JM, Sirianni RW, Stabenfeldt SE, Hyaluronic acid-laminin hydrogels increase neural stem cell transplant retention and migratory response to SDF-1alpha, Matrix Biol 60–61 (2017) 206–216.

[36]. Arulmoli J, Wright HJ, Phan DTT, Sheth U, Que RA, Botten GA, Keating M, Botvinick EL, Pathak MM, Zarembinski TI, Yanni DS, Razorenova OV, Hughes CCW, Flanagan LA, Combination scaffolds of salmon fibrin, hyaluronic acid, and laminin for human neural stem cell and vascular tissue engineering, Acta Biomater 43 (2016) 122–138. [PubMed: 27475528]

[37]. Marquardt L, Willits RK, Student award winner in the undergraduate's degree category for the Society for Biomaterials 35th Annual Meeting, Orlando, Florida, April 13–16, 2011. Neurite growth in PEG gels: effect of mechanical stiffness and laminin concentration, J Biomed Mater Res A 98(1) (2011) 1–6. [PubMed: 21538826]

[38]. Swindle-Reilly KE, Papke JB, Kutosky HP, Throm A, Hammer JA, Harkins AB, Willits RK, The impact of laminin on 3D neurite extension in collagen gels, J Neural Eng 9(4) (2012) 046007. [PubMed: 22736189]

[39]. Patterson J, Hubbell JA, Enhanced proteolytic degradation of molecularly engineered PEG hydrogels in response to MMP-1 and MMP-2, Biomaterials 31(30) (2010) 7836–45. [PubMed: 20667588]

[40]. Rubinstein M, Colby RH, Polymer physics, Oxford University Press, 2003.

[41]. Flanagan LA, Ju YE, Marg B, Osterfield M, Janmey PA, Neurite branching on deformable substrates, Neuroreport 13(18) (2002) 2411–5. [PubMed: 12499839]

[42]. Engler AJ, Sen S, Sweeney HL, Discher DE, Matrix elasticity directs stem cell lineage specification, Cell 126(4) (2006) 677–89. [PubMed: 16923388]

[43]. Georges PC, Miller WJ, Meaney DF, Sawyer ES, Janmey PA, Matrices with compliance comparable to that of brain tissue select neuronal over glial growth in mixed cortical cultures, Biophys J 90(8) (2006) 3012–8. [PubMed: 16461391]

[44]. Saha K, Keung AJ, Irwin EF, Li Y, Little L, Schaffer DV, Healy KE, Substrate modulus directs neural stem cell behavior, Biophys. J 95(9) (2008) 4426–38. [PubMed: 18658232]

[45]. Banerjee A, Arha M, Choudhary S, Ashton RS, Bhatia SR, Schaffer DV, Kane RS, The influence of hydrogel modulus on the proliferation and differentiation of encapsulated neural stem cells, Biomaterials 30(27) (2009) 4695–9. [PubMed: 19539367]

[46]. Hynes SR, Rauch MF, Bertram JP, Lavik EB, A library of tunable poly(ethylene glycol)/poly(L-lysine) hydrogels to investigate the material cues that influence neural stem cell differentiation, J Biomed Mater Res A 89(2) (2009) 499–509. [PubMed: 18435406]

[47]. Laundos TL, Silva J, Assuncao M, Quelhas P, Monteiro C, Oliveira C, Oliveira MJ, Pego AP, Amaral IF, Rotary orbital suspension culture of embryonic stem cell-derived neural stem/progenitor cells: impact of hydrodynamic culture on aggregate yield, morphology and cell phenotype, J Tissue Eng Regen Med 11(8) (2017) 2227–2240. [PubMed: 26880706]

[48]. Bento AR, Quelhas P, Oliveira MJ, Pego AP, Amaral IF, Three-dimensional culture of single embryonic stem-derived neural/stem progenitor cells in fibrin hydrogels: neuronal network formation and matrix remodelling, J Tissue Eng Regen Med 11(12) (2017) 3494–3507. [PubMed: 28032468]

[49]. Darling NJ, Hung YS, Sharma S, Segura T, Controlling the kinetics of thiol-maleimide Michael-type addition gelation kinetics for the generation of homogenous poly(ethylene glycol) hydrogels, Biomaterials 101 (2016) 199–206. [PubMed: 27289380]

[50]. Onuma K, Kanzaki N, Size Distribution and Intermolecular Interaction of Laminin-1 in Physiological Solutions, J. Phys. Chem 107 (2003) 11799–11804.

[51]. Hjort M, Bauer M, Gunnarsson S, Marsell E, Zakharov AA, Karlsson G, Sanfins E, Prinz CN, Wallenberg R, Cedervall T, Mikkelsen A, Electron microscopy imaging of proteins on gallium phosphide semiconductor nanowires, Nanoscale 8(7) (2016) 3936–43. [PubMed: 26838122]

[52]. Lampe KJ, Mooney RG, Bjugstad KB, Mahoney MJ, Effect of macromer weight percent on neural cell growth in 2D and 3D nondegradable PEG hydrogel culture, J Biomed Mater Res A 94(4) (2010) 1162–71. [PubMed: 20694983]

[53]. I.O.f. Standardization, ISO 10993–5:2009 : Biological evaluation of medical devices Tests for in vitro cytotoxicity, 2009.

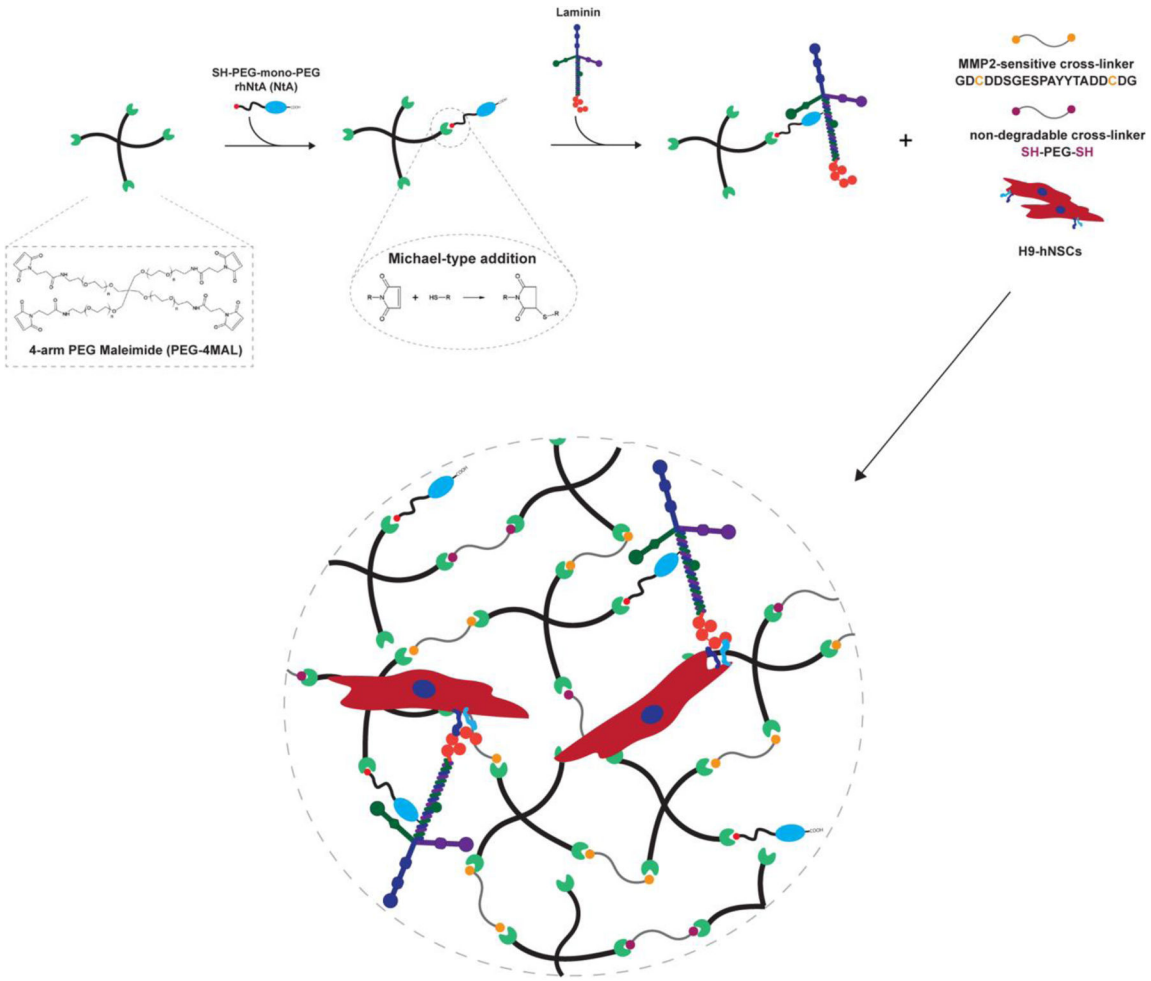

Figure 1. Schematic representation of the preparation of cell-laden affinity-bound laminin PEG-4MAL hydrogels (not to scale).

PEG-4MAL macromer is firstly functionalized with a thiol-containing mono-PEGylated rhNtA (NtA) domain, which will then mediate the binding of laminin with high affinity. Functionalized PEG-4MAL is then reacted with a mixture of protease degradable (MMP2-sensitive peptide) and non-degradable (PEG-dithiol) cross-linkers to allow the formation, under physiological conditions, of a hydrogel network in the presence of cells.

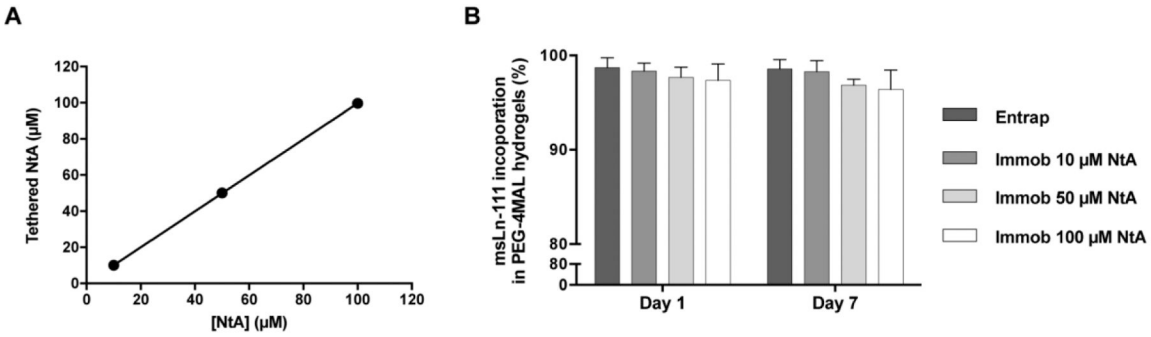

Figure 2. Effect of NtA concentration on laminin incorporation A)

Density of NtA tethered to PEG-4MAL hydrogel as a function of input NtA concentration. Linear regression: $y = 0.9954\ x + 0.1115$; $R^2 = 0.9999$. Data represent mean ± standard deviation (SD) of three hydrogels prepared independently. **B)** Laminin incorporation by physical entrapment (Entrap) or by immobilization using an affinity binding ligand (Immob) into PEG hydrogels, determined by ELISA, after 1 and 7 days of incubation in PBS. Data represent mean ± SD of three hydrogels prepared independently. No significant differences were detected (two-way ANOVA).

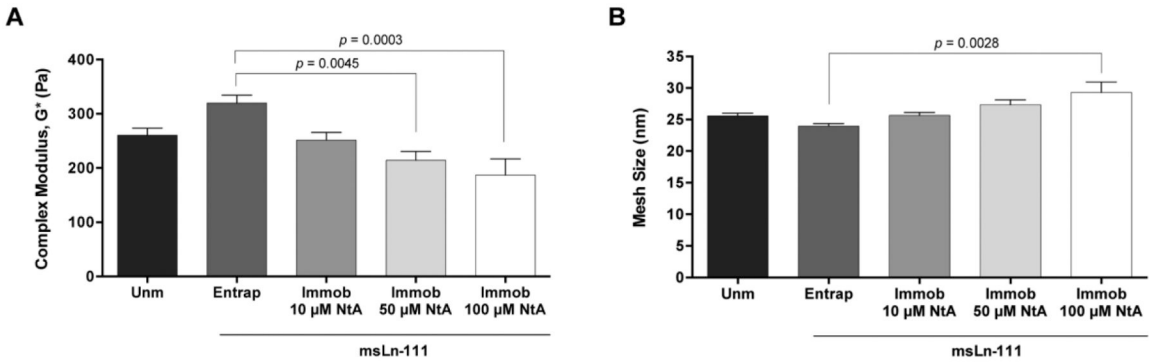

Figure 3. Mechanical and structural properties of PEG-4MAL hydrogels modified with affinity-bound laminin.

A) Complex modulus (G*) of hydrogels determined by rheological analysis; and B) Estimation of hydrogels mesh size, based on the measured storage modulus (G'). Data represent mean ± SEM; n = 6; one-way ANOVA followed by Bonferroni's test.

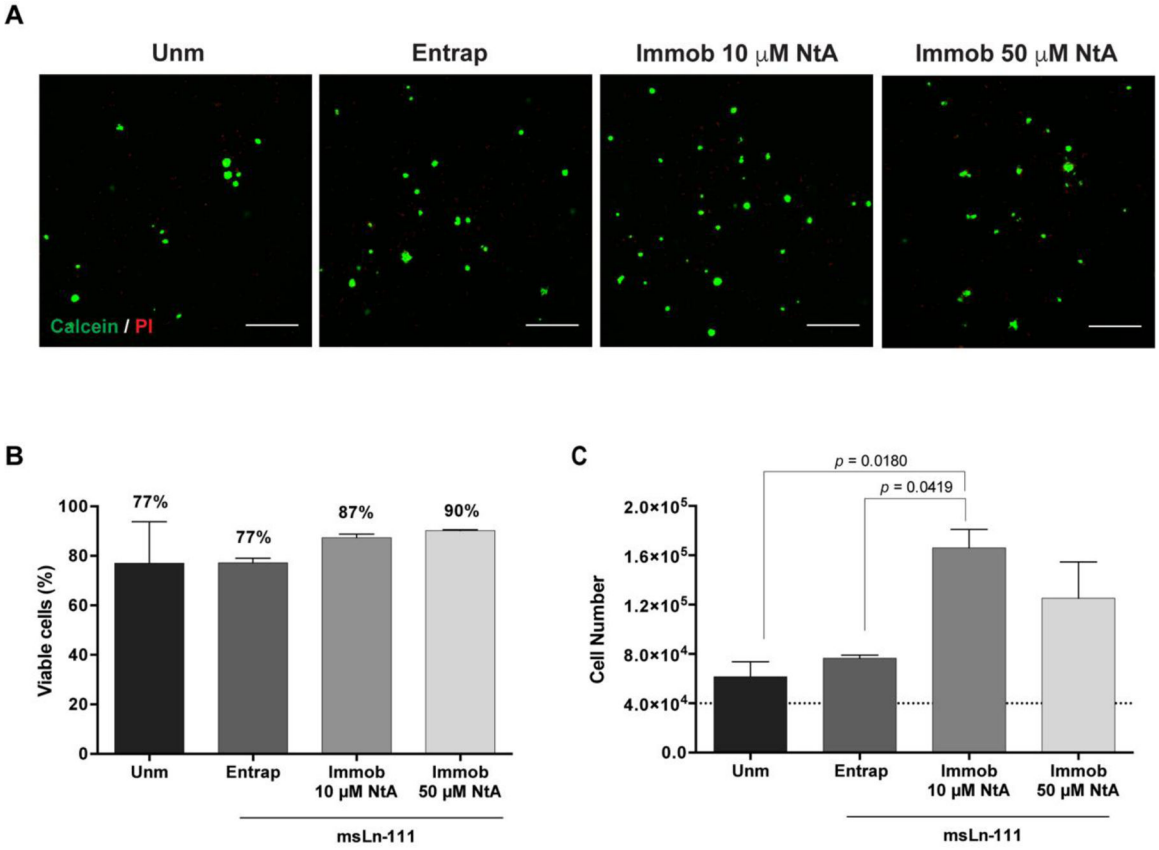

Figure 4. Ability of affinity-bound laminin to support hNSC viability and proliferation.

A) Representative 2D projections of CLSM 3D stack images of cell-laden hydrogels covering a thickness of 300 μm, showing the distribution of live (in green) and dead (in red) cells at day 7 of cell culture. Scale bar = 300 μm. **B)** Quantitative analysis of live cells at day 7, as determined by flow cytometry. Data represent mean ± SD of three independent experiments. No significant differences were detected (one-way ANOVA followed by Bonferroni's test). **C)** Quantitative analysis of total cell number at day 7, as determined by CyQuant® Cell Proliferation kit. The dotted line represents the initial cell density/hydrogel (4×10^4 cells/hydrogel). Data represent mean ± SEM of three independent experiments performed in triplicate; one-way ANOVA followed by Bonferroni's test.

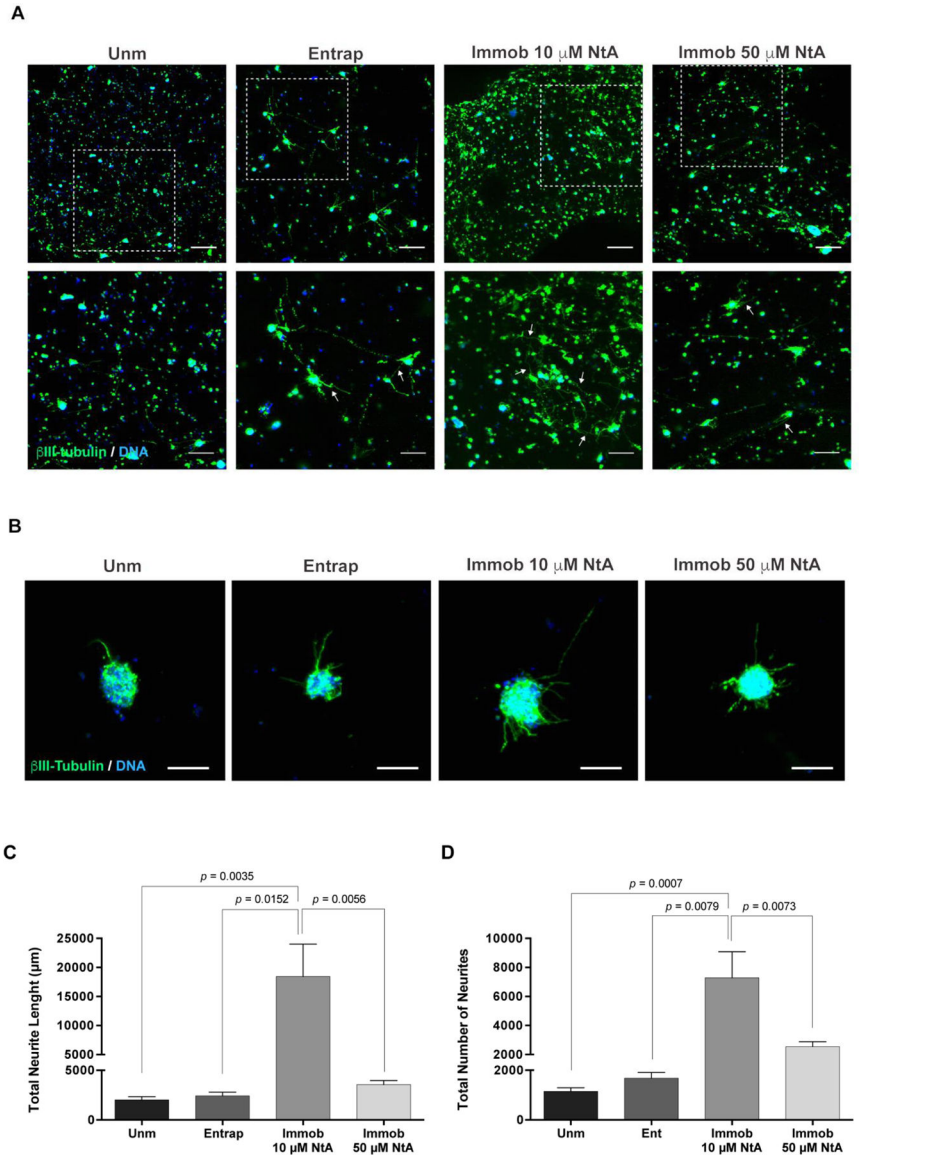

Figure 5. Affinity-bound laminin PEG-4MAL hydrogels and their effect on hNSC neurite outgrowth.

A) hNSC cultured for 14 days within unmodified (Unm), physically entrapped laminin (Entrap) or NtA affinity-bound laminin (Immob) PEG-4MAL hydrogels. Images show 2D projections of CLSM 3D stack images of cells processed for immunofluorescence labeling of βIII-tubulin/DNA covering a thickness of 200 μm (top images) and 100 μm (bottom images). Lower panels show magnified views of selected regions highlighted by dashed squares in the upper panel. Arrows depict neurites expressing βIII-tubulin protruding from neurospheres. Scale Bar = 200 μm (top images); 100 μm (bottom images). **B)** Representative 2D projections of CLSM 3D stack images depicting hNSC outgrowth at day 14 of cell culture, covering a thickness of 80 μm. Scale Bar = 80 μm. **C)** Total Neurite Length; and **D)** Total Number of Neurites determined by quantitative analysis of projected CLSM images. Data represent mean ± SD of 12–15 images analyzed per condition; one-way ANOVA followed by Bonferroni's test.

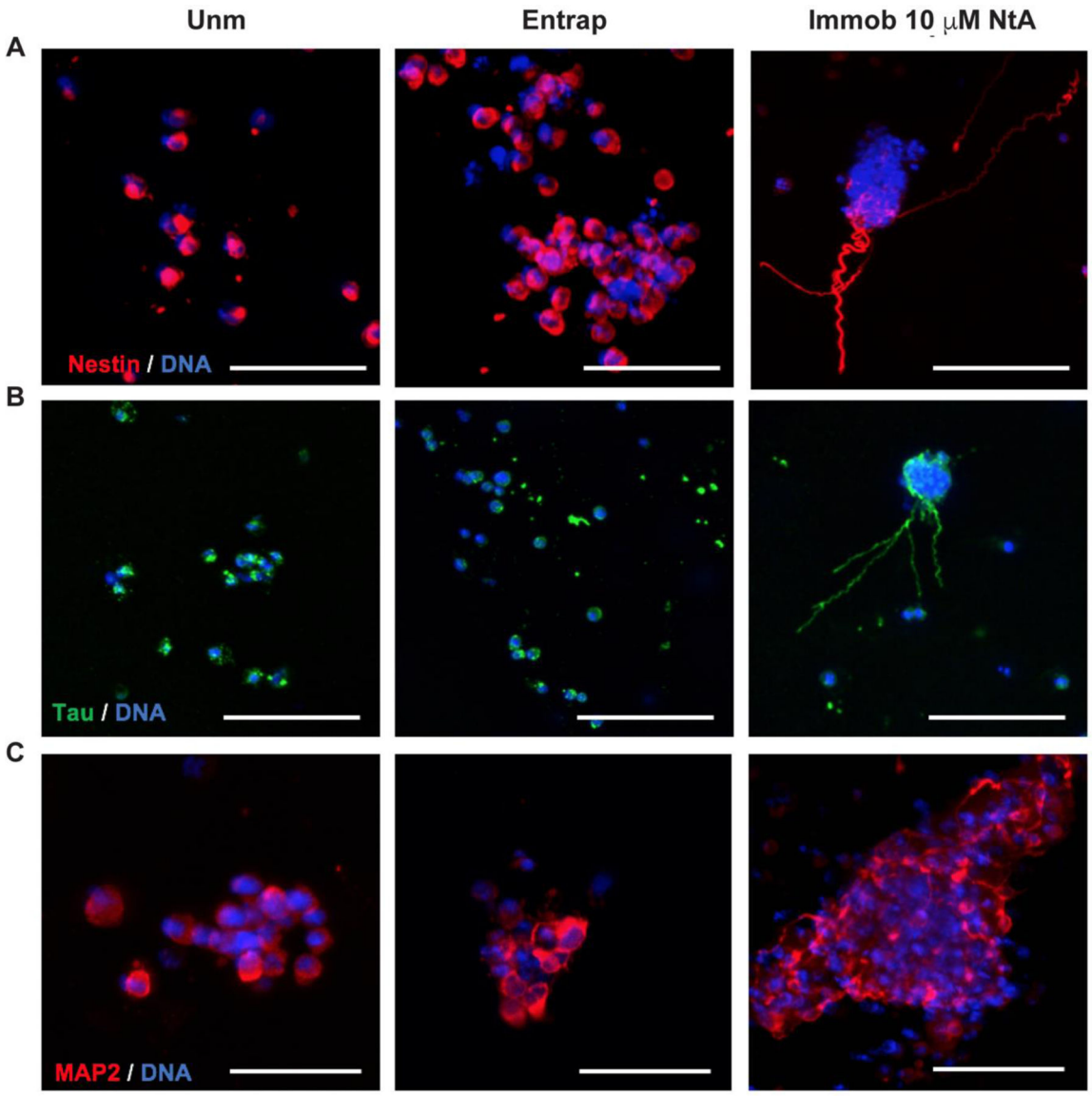

Figure 6. Phenotypic characterization of hNSC within PEG-4MAL hydrogels.

hNSC cultured for 14 days within unmodified (Unm), physically entrapped laminin (Entrap) or NtA affinity-bound laminin (Immob) PEG-4MAL hydrogels. Images show 2D projections of CLSM 3D stack images of cells processed for immunofluorescence labeling of **A)** Nestin; **B)** Tau; and **C)** MAP2. Scale Bar = 100 μm.

Table 1.

Storage modulus (G'), Loss modulus (G") and Phase angle (δ,°) of hydrogels determined by rheological analysis. Data represent mean ± Standard error of the mean (SEM); n = 6.

Hydrogel		Input NtA concentration (μM)	Storage Modulus (G', Pa)	Loss Modulus (G", Pa)	Phase Angle (δ, °)
Unm		–	259.1 ± 13.8	10.6 ± 1.7	2.3 ± 0.2
msLn-111	**Entrap**	–	314.0 ± 16.3	9.3 ± 0.3	2.1 ± 0.1
	Immob	10	256.0 ± 14.2	10.0 ± 0.0	2.3 ± 0.1
		50	213.9 ± 16.4	10.3 ± 1.7	2.8 ± 0.4
		100	187.0 ± 29.5	10.3 ± 0.7	3.7 ± 0.7